Unnatural Parity States in O^{16}. I

D. A. BROMLEY, H. E. GOVE, J. A. KUEHNER, A. E. LITHERLAND, AND E. ALMQVIST
Chalk River Laboratories, Atomic Energy of Canada Limited, Chalk River, Ontario, Canada
(Received December 15, 1958)

A detailed study of the de-excitation of gamma emitting states in O^{16} at 8.87, 10.94, and 11.06 Mev has been carried out using the $N^{14}(He^3,p\gamma)O^{16}$ reaction. Branching ratios and angular distribution measurements on both proton groups and gamma radiations strongly suggest assignments 2^-, 0^-, and 3^+, respectively, although in the latter case the 2^- possibility is not excluded. The experimental results are compared with predictions of the alpha-particle and intermediate-coupling shell models. While considerable areas of agreement exist, serious discrepancies remain in both cases. The identification of the 0^-, 10.94-Mev state precludes Dennison's preferred "identification (a)" in the alpha-particle model and fixes the exchange mixture in the shell model calculations; the O^{16} mixture closely resembles a Serber rather than the Rosenfeld mixture commonly in use in these shell model calculations. From the measured de-excitation branching ratio $\Gamma_\alpha/\Gamma_\gamma$ for the 10.94-Mev state and the systematics of gamma-radiation and alpha-particle transition widths, an upper limit of $\sim 2\times 10^{-9}$ is obtained for the relative intensity of an opposite-parity component in the wave function of this state.

INTRODUCTION

THE O^{16} level structure has been the object of recent extensive investigation, both experimental and theoretical; these investigations have, in part at least, been motivated by the anticipation of particular symmetry effects resulting from the doubly-magic configuration of this nucleus.

This paper and the following one[1] present the results of a series of investigations carried out via the $N^{14}(He^3,p\gamma)O^{16}$ and $N^{14}(He^3,p\gamma\gamma)O^{16}$ reactions. This paper will be concerned chiefly with the direct measurements on the proton and gamma-ray spectra and with proton-gamma coincidence measurements performed to elucidate the electromagnetic de-excitation of certain of the O^{16} states. These results, together with those to be presented in II on the gamma-gamma angular correlations, have been presented in summary previously.[2–4]

The available experimental information up to 1955 on the O^{16} nucleus has been summarized in the review article of Ajzenberg and Lauritsen.[5] In a detailed study of the $N^{16}(\beta^-)O^{16}$ decay and the $F^{19}(p,\alpha\gamma)O^{16}$ reaction Wilkinson, Toppel, and Alburger[6] have demonstrated the existence of a state in O^{16} at 8.87 Mev to which they make the assignment 2^-. Measurements to be described herein and in II fix this assignment and, together with those of Bent and Kruse[7] and of Wakatsuki *et al.*[8] on the $F^{19}(p,\alpha\gamma)O^{16}$ reaction, provide further information on the gamma de-excitation of this state.

Hornyak and Sherr,[9] in a study of the inelastic scattering of 19-Mev protons on O^{16}, present evidence for a state having an appreciable gamma de-excitation width at 11.08 ± 0.03 Mev excitation. Magnetic spectrograph measurements of Squires *et al.*[10] located a state at 11.085 ± 0.014 Mev. Because of its finite gamma width this state was presumed to have "unnatural" parity [i.e., $\pi=(-1)^{J+1}$] and therefore to be not identical with the level seen at roughly this excitation in the work of Bittner and Moffat[11] on elastic scattering of alpha particles from C^{12}.

Early measurements in this latoratory[2–4] on the energies of the de-excitation gamma radiation from the levels in the vicinity of 11 Mev were not consistent, within the extimated precision of the measurements, with the existence of only a single gamma-emitting level in this region. This difficulty was relsolved by Wiel, Jones, and Lidofsky[12] who measured thresholds in the $N^{15}(d,n)O^{16}$ reaction corresponding to the presence of excited states in O^{16} at excitations of 10.935 ± 0.010 and 11.061 ± 0.015 Mev. Further measurements on the de-excitation of the lower of these levels have been made by Wakatsuki and co-workers[8] and by Bent and Kruse.[7] The experimental data now available will be summarized later in this paper.

One of the first theoretical treatments of the O^{16} level spectrum is that of Dennison[13] based on the alpha-particle model; i.e., a semirigid tetrahedral structure consisting of the four alpha-particle substructures with harmonic relative binding. This first treatment was remarkably successful in correlating the available information on the low $(T=0)$ levels. With the discovery and identification of further levels,

[1] Kuehner, Litherland, Almqvist, Bromley, and Gove, following paper [Phys. Rev. **114**, 775 (1959)]; hereafter referred to as II.
[2] Bromley, Ferguson, Gove, Litherland, and Almqvist, Bull. Am. Phys. Soc. Ser. II, **2**, 51 (1957).
[3] Litherland, Almqvist, Bromley, Gove, and Ferguson, Bull. Am. Phys. Soc. Ser. II, **2**, 51 (1957).
[4] D. A. Bromley, in *Proceedings of the Rehovoth Conference on Nuclear Structure*, edited by H. J. Lipkin (North-Holland Publishing Company, Amsterdam, 1958).
[5] A. Ajzenberg and T. Lauritsen, Revs. Modern Phys. **27**, 77 (1955).
[6] Wilkinson, Toppel, and Alburger, Phys. Rev. **101**, 673 (1956).
[7] R. D. Bent and T. H. Kruse, Phys. Rev. **108**, 802 (1957).
[8] Wakatsuki, Hirao, Okada, and Muira, J. Phys. Soc. Japan **12**, 1178 (1957).
[9] W. F. Hornyak and R. Sherr, Phys. Rev. **100**, 1409 (1955).
[10] Squires, Bockelman, and Buechner, Phys. Rev. **104**, 413 (1956).
[11] J. W. Bittner and R. D. Moffat, Phys. Rev. **96**, 374 (1954).
[12] Weil, Jones, and Lidofsky, Phys. Rev. **108**, 800 (1957).
[13] D. M. Dennison, Phys. Rev. **57**, 454 (1940).

this model has been revised by Dennison[14] and more recently extended to higher excitations by Kameny.[15] While a remarkably good qualitative agreement has been obtained, there are outstanding difficulties with the model which will be discussed later in more detail.

Elliott and Flowers[16] have carried out a detailed, intermediate-coupling shell model calculation of the negative-parity level spectrum of O^{16} arising from the removal of a $1p$ nucleon from the closed p shell core into the $p^{-1}d$ and $p^{-1}2s$ configurations. A number of predictions arising from these calculations will be compared with the experimental data later in this paper. Although *a priori* the alpha-particle model and the shell model appear to have little in common other than comparable agreement with the experimental observations, Perring and Skyrme[17] have succeeded in demonstrating that the wave functions for the ground and 6.06-Mev states in O^{16} given by the two models are essentially identical. Further investigation of the connection between these models would be of particular interest.

It has generally been assumed that a simple shell model is inadequate to describe the low positive-parity states of O^{16} since multiple nucleon excitation would be required to give this parity. It has been customary, for example, to represent the 6.06-Mev 0^+ state as a configuration wherein 2 nucleons were raised into the s and d shells; this, within the usual shell model framework, would require 10–15 Mev per nucleon and would appear to be an untenable assumption. Ferrell and Visscher[18] have noted that single nucleon excitation to the next higher negative-parity shell requires comparable energy and have considered the interpretation of the positive-parity states on this basis together with the possibility of spheroidal deformation of the system.

Morinaga[19] has investigated, in some detail, the consequences of assuming the "hole configuration" suggested by Christy and Fowler[20] wherein four p nucleons are lifted simulataneously into the s and d shells, in an attempt to correlate the observational data on the positive-parity levels. Griffin,[21] using the method of Generator Coordinates, has examined the problem of the dilational and collective quadrupole excitations of the O^{16} structure to make predictions regarding the location of 0^+ and 2^+ levels, respectively.

In experimental studies of the gamma-emitting or unnatural-parity states of O^{16}, the major difficulty is usually that of resolving the gamma transitions of interest from a high background of gamma radiation

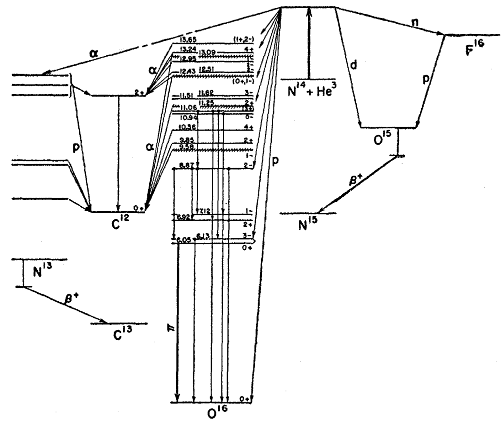

FIG. 1. Schematic representation of the reactions induced by He^3 bombardment of N^{14}.

resulting from competing open channels. The $N^{14}(He^3,p\gamma)O^{16}$ reaction is particularly suited to a study of these states since, as indicated in Fig. 1, almost all other channels, open for low bombarding energies, lead to final levels which are unstable to particle emission and which therefore do not contribute appreciably to the gamma radiation yield. This reaction has the further advantage that the high-energy proton groups leading to the states of interest are readily detected, permitting the study of $(p\gamma)$ coincidences to establish de-excitation branching ratios. The high Q value, as listed below, also results in the attainment of high excitations in O^{16} with relatively low incident energies. The exceptions among the final levels formed are the 4.43-Mev level in C^{12} formed in the $N^{14}(He^3,p\alpha\gamma)C^{12}$ reaction via the higher states in O^{16}, or in the $N^{14}(He^3,\alpha,p\gamma)C^{12}$ reaction via the higher states in N^{13} and the ground states of N^{13} and O^{15} which have 0.511-Mev annihilation radiation associated with their positron decay. The Q values, as calculated from the mass tabulation of Mattauch *et al.*,[22,23] are the following:

$$\begin{aligned} N^{14}+He^3 \rightarrow F^{17*} &\rightarrow F^{17}+h\nu+15.826 \text{ Mev} \\ &\rightarrow F^{16}+n-1.129 \text{ Mev} \\ &\rightarrow O^{16}+p+15.231 \text{ Mev} \\ &\rightarrow O^{15}+d+1.861 \text{ Mev} \\ &\rightarrow O^{14}+t-5.171 \text{ Mev} \\ &\rightarrow N^{13}+\alpha+10.029 \text{ Mev.} \end{aligned}$$

Because of the high compound-system excitation and the large number of open particle channels, radiative capture of the incident He^3 ions would not be expected to be detectable. A search for radiative He^3 capture in the particularly favorable case of He^3 on O^{16} has yielded

[14] D. M. Dennison, Phys. Rev. **96**, 378 (1954).
[15] S. L. Kameny, Phys. Rev. **103**, 358 (1956).
[16] J. P. Elliott and B. H. Flowers, Proc. Roy. Soc. London **A242**, 57 (1957).
[17] J. K. Perring and T. H. R. Skyrme, Proc. Phys. Soc. London **A69**, 600 (1956).
[18] R. A. Ferrell and W. M. Visscher, Phys. Rev. **102**, 450 (1956).
[19] H. Morinaga, Phys. Rev. **101**, 254 (1956).
[20] R. F. Christy and W. A. Fowler, Phys. Rev. **96**, 851 (1954).
[21] J. J. Griffin, Phys. Rev. **108**, 328 (1957).
[22] Mattauch, Waldmann, Bieri, and Everling, Z. Naturforsch. **11**, 525 (1956); *Annual Review of Nuclear Science* (Annual Reviews, Inc., Palo Alto, California, 1956), Vol. 6.
[23] D. A. Bromley and A. R. Rutledge, Chalk River Report CRP-789 (unpublished).

negative results.[24] Nonresonant, direct capture of He^4 by He^3 has been observed[25]; in this case there are no open competing channels.

EQUIPMENT

Much of the experimental equipment used in this work has been described in previous publications. Proton groups were detected using CsI(Tl) crystal spectrometers[26] or a 180° Kellogg-type magnetic analyzer[27]; gamma spectrometers comprising 5-in. diameter by 4-in. long NaI(Tl) crystals[28] were used. Conventional fast-slow coincidence circuits[29] have been used for both $(p\gamma)$ and $(\gamma\gamma)$ coincidence measurements with a coincidence resolving time $2\tau \sim 40$ mμsec; 120- and 100- channel Hutchinson-Scarrott[30] type pulse-height analyzers have been used in recording the data. The "self-coincidence" feature previously reported[26] has been extensively used in establishing voltage gates for coincidence measurements. Total beam charge delivered to the targets was measured with a precision integrator circuit.[26]

As a result of the relatively low yields encountered in these studies and the consequent long run durations required coincidence studies, a simple two-dimensional display circuit has been developed for use with the multichanael analyzers. This system will be described in detail elsewhere[31]; in essence, its operation is to add an appropriate voltage pedestal to a given output pulse from one detector if, and only if, this pulse is in fast-coincidence with a pulse of selected amplitude in a second detector. A number of these pedestals may be adjusted in amplitude so that it is possible to display simultaneously on the multichannel analyzer the spectra from one detector in coincidence with a number of different voltage gates set on that from the other. The number of such simultaneous spectra is limited only by the maximum number of channels available and the minimum number required to resolve the structure in a particular coincidence spectrum. Examples of the use of this circuit appear later in Figs. 14 and 15 where 3 and 2 simultaneous gates have been used, respectively. Not only does this use of the Pedestal Insertion Gate (PIG) circuit permit a more economical utilization of accelerator time but also it obviates the possibility of errors in relative normalization, beam integration, or target condition.

In examining the particle angular distributions with the CsI spectrometers, a standard 17° tilted axis chamber[32] was used permitting detector rotation from −145° to 0 to +145° in the laboratory system. With the Kellogg magnet a continuous rotation chamber[33] has been used which permits rotation of the detector in a horitontal plane from −40° to +145°.

TARGET PREPARATION

Targets of Wolfram and tantalum nitride have been used in these measurements. These have been produced by induction heating of cleaned 0.020- and 0.010-inch blanks in nitrogenous atmospheres. It has been found that boiling the target blanks in an aqueous solution of "Alconox"[34] commercial cleaner followed by distilled water rinses provides substantial freedom from contaminant layers. The technique evolved for the production of the nitride targets involves heating the blank to approximately 1200°C in an atmosphere of NH_3 and NH_4OH for 10 seconds at an original gas pressure of 4 inches Hg. It has been found that dry NH_3, mixtures of N_2 and H_2 and pure N_2 give progressively less satisfactory nitride formation. In the case of an NH_3+NH_4OH atmosphere the quoted 1200°C represents an optimum, but not particularly critical value; with an N_2 atmosphere the temperature control is relatively critical and proper nitride formation appears to take place only in the range from 725 to 850°C.

It is perhaps worth recording that nitrogen targets produced by induction nitriding of thin evaporated layers of Al, Mg, Sr, and Ca on heavy-element backings proved unsatisfactory because of low nitride as opposed to oxide formation. Evaporated Na(CN) targets gave high specific nitrogen concentration but had the major disadvantages of short life under bombardment and built-in carbon contamination.

In order to examine the structure of the nitride surface and estimate the effective target thickness, the yield of 4.43-Mev radiation from the $N^{15}(p,\alpha\gamma)C^{12}$ reaction on the natural N^{15} component in the targets was examined in the vicinity of the 2^- resonance at 898-kev bombarding energy.[35] Figure 2 is a typical yield curve so obtained. The fact that the yield step rises to its full height in a proton energy interval comparable to the measured 2.2-kev width of the

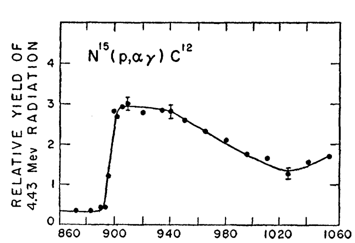

FIG. 2. Yield of 4.43-Mev radiation from the reaction $N^{15}(p,\alpha\gamma)C^{12}$ in the vicinity of the 898-kev resonance.

[24] Bromley, Kuehner, and Almqvist, Bull. Am. Phys. Soc. Ser. II, 3, 199 (1958), and to be published.
[25] H. D. Holmgren and R. L. Johnston, Bull. Am. Phys. Soc. Ser. II, 3, 26 (1958), and private communication.
[26] Bromley, Almqvist, Gove, Litherland, Paul, and Ferguson, Phys. Rev. **105**, 957 (1957).
[27] Snyder, Rubin, Fowler, and Lauritsen, Rev. Sci. Instr. **21**, 852 (1950).
[28] Litherland, Paul, Bartholomew, and Gove, Phys. Rev. **102**, 208 (1956).
[29] Graham, Bell, and Petch, Can. J. Phys. **30**, 35 (1952).
[30] G. W. Hutchinson and G. G. Scarrott, Phil. Mag. **42**, 792 (1951).
[31] A. E. Litherland and D. A. Bromley (to be published).
[32] R. L. Clarke and E. B. Paul, Can. J. Phys. **35**, 155 (1957).
[33] R. L. Clarke (to be published).
[34] Available from Alconox Inc., Jersey City, New Jersey.
[35] A. A. Kraus, Jr., Phys. Rev. **94**, 975 (1954); **89**, 299 (1953).

resonance indicates that the nitride target layer is quite uniform. Using the standard expression for a "thick" target yield step,[27] i.e.,

$$Y=(\pi/2)(\sigma\Gamma/\epsilon),$$

where Γ is the resonance width,[5] σ the cross section (800 mb),[5] and ϵ the molecular stopping cross section for TaN^{15} obtained from the N^{15} isotopic abundance[36] and Whaling's compilation[37] of stopping cross sections as 7.94×10^{-15} kev cm^2, the predicted yield step agrees with that observed to within a factor of three. The discrepancy is in the direction to be expected if the nitride layer were slightly diluted with Ta atoms as might indeed be expected. These measurements demonstrate, however, that the targets are quite uniform and essentially pure TaN.

From the shape of the observed yield curves (e.g., Fig. 2), effective target thicknesses of $\sim50\pm20$ kev were obtained for 900-kev protons. From this an areal density of TaN of $\sim(1.7\pm0.5)\times10^{18}$ molecules/cm^2 follows. This density is also consistent with $N^{14}(\alpha,\gamma)F^{18}$ measurements[38] carried out using these same targets.

TARGET CONTAMINANTS

Again because of the low yields from He^3 reactions on N^{14} as compared to C^{12}, the inevitable carbon target contamination posed a particularly severe problem. Additional pumping stages in the target line provided inadequate reduction of this contamination. In an attempt to minimize this buildup of carbon, provision was made to cement an electrical strip heater in intimate contact with the target backing, thus making it possible to hold the target at ~500°C during measurements. The heater was energized using a special transformer with Teflon insulation on the secondary winding to permit integration of the beam intercepted by the target. Figure 3 illustrates the effect of this heater on

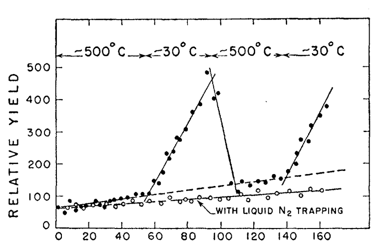

FIG. 3. Buildup of carbon contaminant on a clean tantalum blank. The indicated 500°C temperatures were maintained with a resistance heater attached directly to the target backing. The ordinate scale represents the yieldof 2.31-Mev radiation from the $C^{12}(He^3,p)N^{14}$ reaction at 21-Mev bombarding energy. The time scale is measured from the initiation of bombardment. The target heater was not in use during the measurement with liquid nitrogen trapping.

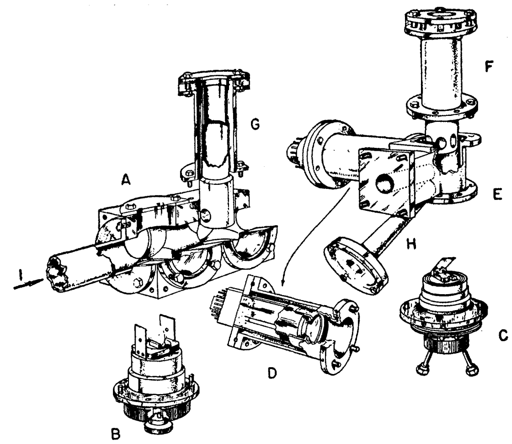

FIG. 4. Schematic drawing of the target structure in use. All flange dimensions, etc., have been standardized to allow considerable flexibility in assembly. The ion beam I from the accelerator enters the basic block structure A, and its cross section is defined as or if required by the aperture block and retractable quartz viewer unit B. Following this, it traverses a liquid nitrogen trap G and enters an auxiliary target chamber E on which the target support mount C and the target shrouding liquid nitrogen trap F are mounted. Particles emitted from the target are detected in a CsI(Tl) spectrometer assembly D; a similar monitor counter may be attached at H. The aperture of the CsI spectrometer is defined by a tantalum baffle mounted directly over the 0.0004-in. aluminum foil which covers the crystal which is in turn optically coupled to an RCA-6655 2-in. photomultiplier by a thin film of silicone vacuum grease. A lead hood shields the crystal and photocathode region of the photomultiplier from low-energy gamma radiation; mu-metal and iron coaxial shield cylinders are provided for the photomultiplier itself. Additional auxiliary chambers similar to E are available which have complete cylindrical symmetry about a vertical axis through the target for use in $(\gamma-\gamma)$ correlation measurements; one of these has been constructed completely of Lucite to minimize the absorption of low-energy gamma radiation in the chamber walls. That shown is used for particle-gamma correlation measurements with the gamma spectrometer swinging out of the plane of the figure. In some correlation measurements reported in this paper the CsI spectrometer replaced the liquid nitrogen trap F to detect particles perpendicular to the plane of motion of the gamma spectrometer.

carbon buildup; plotted is the yield of 2.3-Mev radiation from the $C^{12}(He^3,p\gamma)N^{16}$ reaction as a function of time with a fixed 0.5-μa beam of 2.10-Mev He^3 ions incident on a clean tantalum target backing. The breaks in this curve were produced by periodically interrupting the heater current. It is of interest to note that there are apparently two quite distinct carbon components present; that which can be removed by reconnecting the heater is presumably due to the condensation of organic vapors on the target surface, while the remaining component may represent carbon driven into the target surface by the beam itself.

It was found that the contaminant reduction resulting from the target heating was also inadequate, and following a suggestion of Butler[39] an additional trap attachment was designed for the standard target plumbing in use in order to shroud the target as completely as possible with surfaces maintained at liquid N_2 temperature. This system is illustrated in

[36] A. O. Nier, Phys. Rev. 77, 789 (1950).
[37] W. Whaling, in *Handbuch der Physik* (Springer-Verlag, Berlin, 1958), Vol. 34.
[38] Almqvist, Bromley, and Kuehner, Bull. Am. Phys. Soc. Ser. II, 3, 27 (1958), and to be published.
[39] J. W. Butler (private communication, 1956).

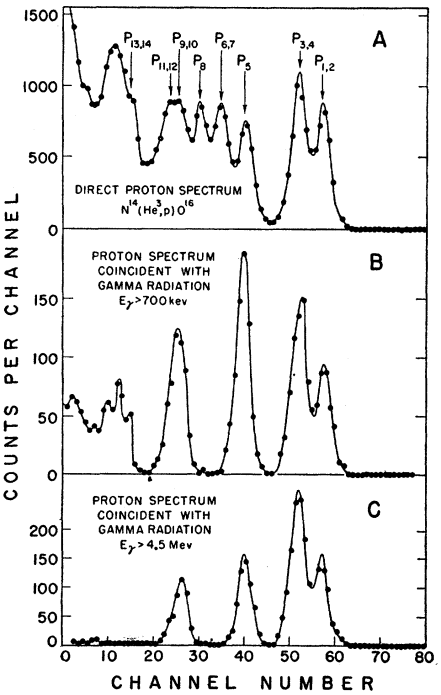

FIG. 5. Proton spectra from the $N^{14}(He^3,p)O^{16}$ reaction obtained in a CsI spectrometer both directly (A) and in coincidence with gamma radiation (B,C).

Fig. 4. As shown in Fig. 3, installation of this trap produced an appreciable reduction in the rate of carbon buildup; simultaneous use of heater and trap resulted in an exorbitant consumption of liquid N_2 and little, if any, reduction in rate beyond that obtained with the trap alone. Use of the target heater was discontinued.

EXPERIMENTAL RESULTS

Proton Spectra

Figure 5 shows proton spectra measured at 90° to the incident 2.1-Mev incident He^3 ion beam. Part A of the figure is the direct spectrum as measured with a CsI spectrometer; the ground-state proton group (p_0) does not appear since the system gain has been adjusted to put it above the upper end of the analyzing range. The instrumental resolution is clearly inadequate to resolve the closely spaced groups; p_5 corresponding to the 8.87-Mev state is resolved however as is p_8 corresponding to the 10.36-Mev state. Parts B and C of this figure show corresponding spectra from the same detector measured in coincidence with gamma radiation detected at 90° to the beam and 180° to the protons with energy greater than 700 kev and 4.5 Mev, respectively. In order to isolate the gamma-emitting states in O^{16}, these limits were chosen to be above the strong 0.511-Mev annihilation radiation and the 4.43-Mev radiation from C^{12}. Reference to the level diagram of Fig. 1 shows that the low-energy proton groups in Part B are those leading to the formation of states which subsequently de-excite by alpha emission to the first excited state of C^{12}. The remaining peaks labelled p_5 and $p_{9,10}$ in the figure then correspond to the unnatural parity states at 8.87 and ~11 Mev; the resolution does not permit the separation of the two groups at the latter energy. The relative peak heights in parts B and C of this figure reflect the nature of the gamma de-excitation of the corresponding state or pair of states; the lack of gamma radiation from the 6.06-Mev state for example depresses the coincidence yield of the p_{12} group.

Figure 6 is an expanded proton spectrum similar to part B of Fig. 5 in coincidence with all gamma radiation with energy greater than 700 kev. As a check on the correctness of the deductions just noted, a voltage gate, shown shaded, was set on the composite proton peak corresponding to states in O^{16} at ~13-Mev excitation and the coincident gamma radiation spectrum, shown in the inset, was obtained. As anticipated, this shows only the 4.43-Mev radiation following alpha emission to the 2^+ state at this energy in C^{12} and the strong contaminant 2.31-Mev radiation from $C^{12}(He^3,p\gamma)N^{14*}$.[26]

The voltage gate shown in this figure via the "self-gate" circuits[26] is typical of those used in obtaining the $(p\gamma)$ coincidence measurements on the p_5 and $p_{9,10}$ groups in that these were set and checked in coincidence with gamma radiation in order to more precisely locate the groups of interest. No evidence was found for any gamma de-excitation branch in coincidence with such a voltage gate set on p_8 to the 10.36-Mev state as might be expected from its 4^+ assignment which allows alpha de-excitation in competition.

Figure 7 shows the result of an examination of the region of the proton spectrum corresponding to 11–12 Mev excitation in O^{16} using a 180° Kellogg-type magnetic analyzer[27] at 90° to a 2.7-Mev He^3 beam. The ground and first excited state proton groups from the contaminant reaction $C^{12}(He^3,p)N^{14}$ [26] are conveniently close to the oxygen doublet and serve as calibration points. Assuming a Q value of 4.767 Mev for the $C^{12}(He^3,p)N^{14}$ reaction as computed from the mass values[23] and Bockelman's determination of the excitation of the first excited state of N^{14},[40] the p_0 and p_1 groups from carbon have energies of 6.413 and 4.258 Mev, respectively, at the bombarding energy and angle used. Using these values to calibrate the magnet energy scale, the peaks at A, B, C, and D correspond to excitations of 11.565, 11.286, 11.127, and 10.981 Mev, respectively; the Q value for the $N^{14}(He^3,p)O^{16}$ reaction of 15.231 Mev has again been taken from the mass values.[23] It should be borne in mind that the carbon target involved here is the very thin contaminant layer on the target surface; consequently the excitations just quoted must be corrected

[40] Bockelman, Brown, Buechner, and Sperduto, Phys. Rev. 92, 665 (1953).

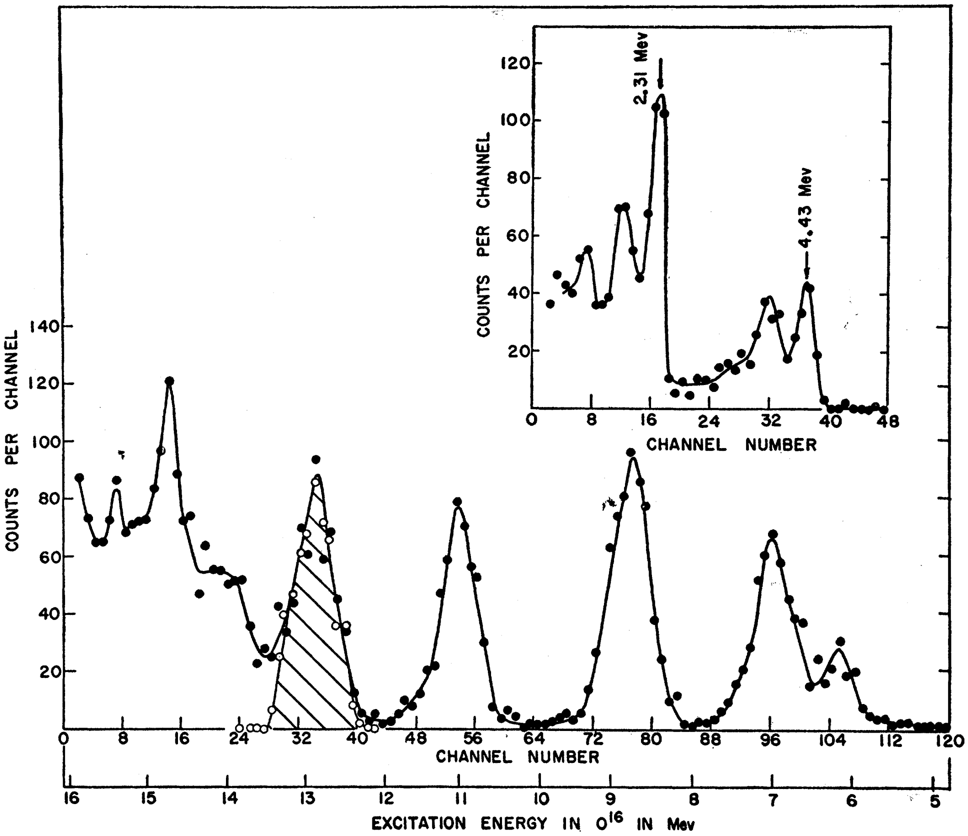

FIG. 6. Proton spectrum coincident with all gamma radiation with $E_\gamma > 700$ kev, showing a typical self-gate display of a coincidence voltage gate set on proton groups to states in O^{16} near 12.5 Mev and the coincident gamma spectrum (insert) from the $N^{14}(He^3, p\alpha\gamma)C^{12}$ reaction.

downwards to correct for the effect of the thicker TaN^{14} target layer. It would be extremely difficult to make a precise correction for this effect with the targets in use. It should be noted, however, that if 40 kev is subtracted from all four excitations quoted (i.e., the calibration is shifted by that amount), the excitations corresponding to peaks A, B, and C would be in excellent agreement with the values 11.250 ± 0.020, 11.510 ± 0.020, and 10.935 ± 0.010 Mev as quoted by Bittner and Moffat[11] from $C^{12}(\alpha,\alpha)C^{12}$ and Weil, Jones, and Lidofsky[12] from $N^{15}(d,n)O^{16}$. The excitation corresponding to peak C would be 11.087 Mev, appreciably higher than that of 11.061 ± 0.015 Mev quoted by Weil *et al.*[12] Since the yield of neutrons to this state in the $N^{15}(d,n)O^{16}$ reaction is very low, this discrepancy may not be a serious one. The present measurement

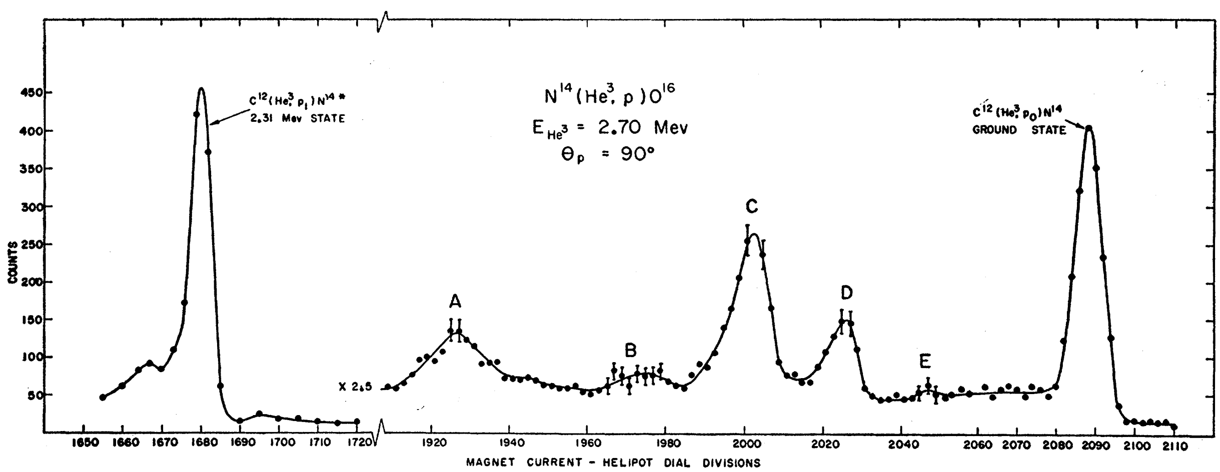

FIG. 7. Proton groups corresponding to excitations in the range 11–12 Mev in O^{16} obtained with a Kellogg-type 180° magnetic spectrometer.

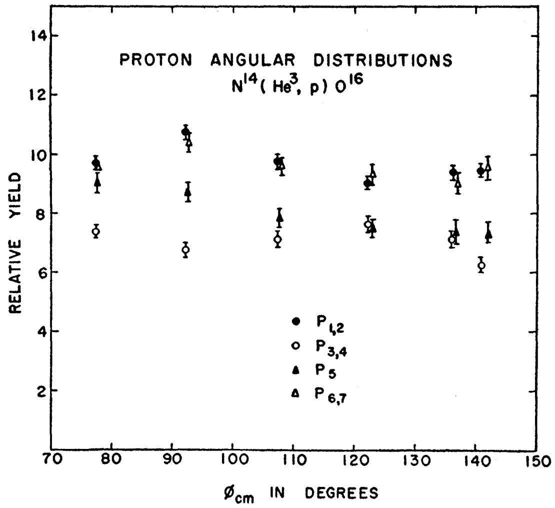

FIG. 8. Angular distributions of proton groups from the reaction $N^{14}(He^3,p)O^{16}$. Angles and intensities have been converted to the center of mass frame.

would locate the second member of the doublet ~11 Mev excitation at 11.087±0.020 Mev relative to the other higher levels in O^{16}; however, the doublet separation is measured with somewhat greater accuracy as 146±10 kev as compared to the value of 126±18 kev measured by Weil *et al.*[12] The energy measurements of the gamma radiation are of course consistent with either excitation value, and for purposes of discussion the earlier values of 10.94 and 11.06 Mev have been retained for these unnatural parity states. The present measurements clearly corroborate the existence of the doublet. It should be emphasized that no direct evidence exists that the state observed in the $N^{15}(d,n)O^{16}$ reaction[12] is that from which de-excitation gamma radiation is observed; the fact that the excitation energy reported here is in agreement with the results of Hornyak and Sherr[9] and of Squires *et al.*[10] suggests the possibility that a triplet of states is present at ~11 Mev in O^{16} and that the level at 11.061 Mev is, in fact, the natural parity state observed by Bittner and Moffat[11] in the alpha-scattering measurements.

The possibility of this or of additional states in this region of excitation in O^{16} is not precluded by the magnetic spectrometer results reported here; the statistical accuracy of the present data is not sufficiently great to suggest the interpretation of weak peaks such as that at E (which would correspond to an excitation in O^{16} of 10.817±0.020 Mev) as evidence for the existence of these states.

Because of the low detection efficiency (7×10^{-4} sphere)[27] as compared to the CsI spectrometers (0.4%)[26] and the low yield from the N^{14} targets, no successful $(p\gamma)$ coincidence measurements have been made using magnetic analysis of the protons. Further, the time which would have been required even for the measurement of the direct particle angular distributions was exorbitant; the magnet was therefore replaced with a CsI spectrometer in obtaining these distributions.

TABLE I. 90° Differential and total cross sections for the $N^{14}(He^3,p)O^{16}$ reaction to low states in O^{16} for 2.10-Mev incident He^3 ions.

Proton group	Excitation in O^{16}	$(J\pi)_f$	$d\sigma/d\omega$ at 90° (μb/sterad)	σ_T (μb/sterad)
p_0	ground state	0^+	4.6	58
p_1+p_2	6.06+6.13	0^+, 3^-	25.2	317
p_3+p_4	6.92+7.12	2^+, 1^-	30.8	387
p_5	8.87	2^-	26.4	332
p_6+p_7	9.58+9.84	1^-, 2^+	39.2	492
p_8	10.36	4^+	30.2	379
p_9+p_{10}	10.94+11.06	0^-, 3^+	37.2	467

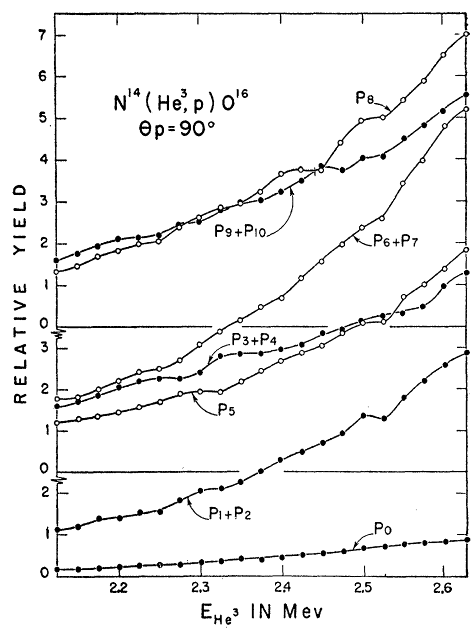

FIG. 9. Excitation curves for proton groups from the reaction $N^{14}(He^3,p)O^{16}$ measured at 90° to the incident He^3 beam.

Data were obtained using only reflection geometry; while nitrogen targets were prepared by nitriding micro-inch nickel foils, it was found that these targets were relatively unstable under He^3 bombardment and that the data were not reproducible from them. Consequently, only data obtained using TaN targets on thick Ta backings are presented.

Figure 8 shows the results obtained; the experimental data have been converted to center-of-mass angles and intensities. Within the experimental accuracy, only the p_5 angular distribution departs from isotropy and in this case by at most 20%.

Figure 9 shows the 90° excitation function for a number of the proton groups to low states and unresolved pairs of states in O^{16} as measured with a CsI spectrometer. Table I lists the differential and total cross sections for these groups as obtained from the

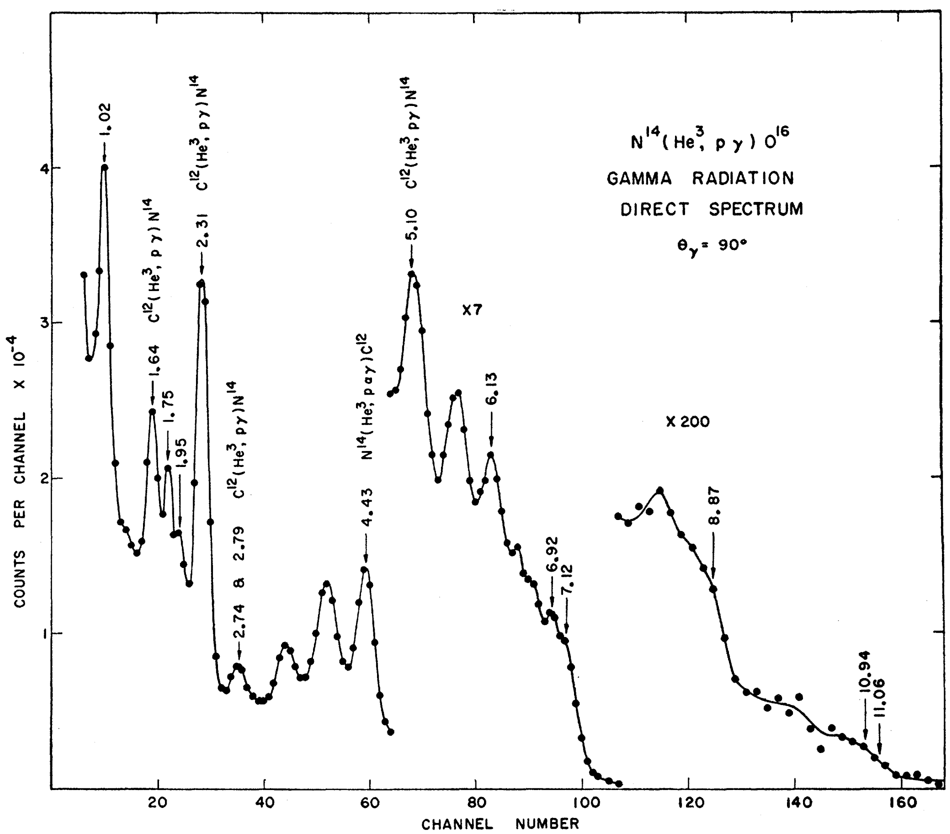

FIG. 10. Direct gamma radiation spectrum from He^3 bombardment of N^{14}. Ordinate expansion factors are shown on the figure. A 5-in. diameter and 4-in. deep NaI crystal at 90° to the incident He^3 beam was used to obtain this spectrum.

target areal density previously quoted, the integrated He^3 current, and the measured efficiency of the proton detectors.[26] It should be emphasized that direct beam integration is only possible where the possibility of significant deuteron contamination in the beam does not exist. The striking feature of these excitation curves is the lack of any marked resonance structure as compared to those for the $C^{12}(He^3,p)N^{14}$ reactions,[23] for example; it should be noted however that as a result of the target thickness $\approx$100-kev sharp resonances, i.e., $\Gamma\sim 10$ kev, if closely spaced, would not be seen in these curves. The compound systems involved are F^{17} and O^{15} at excitations around 18 and 14 Mev, respectively[23]; this lack of resonant structure has important consequences for the interpretation of the gamma-gamma correlation measurements to be discussed in II, as does the isotropy of the proton angular distributions shown in Fig. 9.

Gamma Spectra

Figure 10 is a typical direct spectrum of the gamma radiation associated with the $N^{14}+He^3$ reactions at a bombarding energy of 2.1 Mev. The spectrum is dominated by the 4.43-Mev radiation from the $N^{14}(He^3,p\alpha\gamma)C^{12}$ reaction; the contaminant gamma rays from $C^{12}(He^3,p\gamma)N^{14}$ as indicated on the figure further masked the O^{16} gamma-ray yield so that no detailed intensity measurements are possible on low-energy gamma radiation in the direct spectra. Similar measurements made at various angles to the incident beam demonstrated that again to within the experimental accuracy possible ($\pm15\%$), all the $N^{14}(He^3,p\gamma)O^{16}$ gamma-ray angular distributions were isotropic, a result also of importance to the gamma-gamma correlation interpretation in II.

The direct spectra show a peak at 1.02 Mev corresponding to the simultaneous detection of two 0.511-Mev annihilation quanta and counts corresponding to gamma radiation of energy 8.87 and $\sim$11.0 Mev. In both cases, because of the low intensities involved, it was necessary to investigate the "summation" contribution to these counting rates as distinguished from true contributions corresponding to the de-excitation of states at these energies. These "summation" contributions result when two member gamma radiations from the cascade de-excitation of the state in question enter the gamma spectrometer simultaneously and give a full-energy pulse. Clearly these contributions will be functions of the detector solid angles and of the γ-γ correlations involved in the cascade, vanishing, for example, if the cascade radiations are completely correlated at 180°. A general expression for this correction is derived in Appendix I in terms of the Legendre polynomial coefficients for the γ-γ correlation and the effective angular acceptance of the detectors.

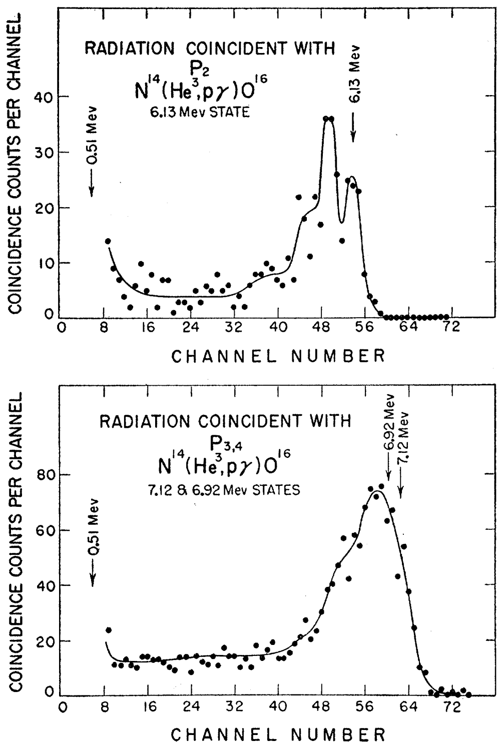

FIG. 11. Gamma radiation spectra coincident with proton groups p_2 and $p_{3,4}$ in the $N^{14}(He^3,p)O^{16}$ reaction. The bombarding energy used was 2.1 Mev.

For the energies and geometry involved in the direct spectrum measurements (Fig. 10), the effective acceptance half-angle θ_0 is $\sim 18°$. The factor $N\epsilon_\gamma$ appearing in the summation contribution Appendix I is simply the singles counting rate for the appropriate cascade gamma ray. The spectrometer efficiencies have been determined previously using calibrated sources and standard coincidence methods[41,42] and have been extrapolated where necessary using the calculations of Wolicki, Jastrow, and Brooks.[43] Using $N\epsilon_{\gamma 1}$ from the spectrum and the measured $\epsilon_{\gamma 2}$ together with R (see Appendix I) obtained from the correlation coefficients listed in II, a summation contribution equal to 10% of the observed counts was calculated for the 8.87-Mev transition; the calculations indicated that all counts corresponding to $\sim$11 Mev could be attributed to the summation process, leaving no evidence for a direct transition of this energy. To check these findings, it was noted that since the direct contribution was given by $N\epsilon_\gamma$ and the summation by $N\epsilon_{\gamma 1}\epsilon_{\gamma 2}$, it was possible to separate the two by observing the counting rates for different ϵ_γ obtained by varying the target-crystal separation. The accuracy of this procedure is considerably reduced over that just described; however, using the variation of ϵ_γ with detector distance as computed by Wolicki *et al.*[43] for the 5-in. crystals, it was again found that all the 11-Mev counts and at most a small fraction of the 8.87-Mev counts could be attributed to summation.

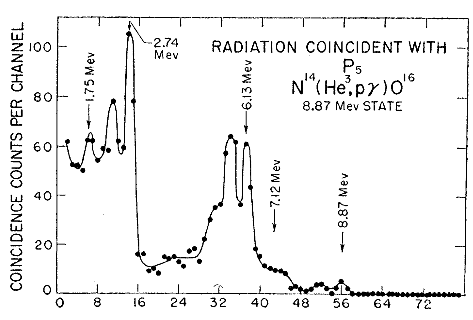

FIG. 12. Gamma radiation spectrum coincident with the proton group p_5 to the 8.87-Mev state in O^{16}, obtained at a bombarding energy of 2.1 Mev.

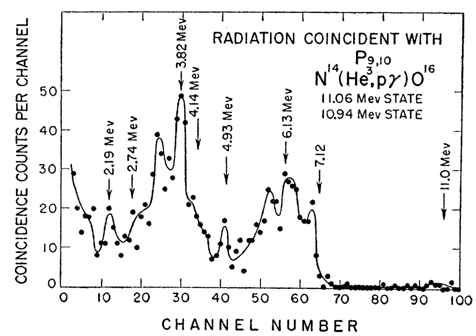

FIG. 13. Gamma radiation spectrum coincident with the composite proton group to the 10.94- and 11.06-Mev states in O^{16} measured at 2.1-Mev incident energy.

p-γ Coincidence Measurements

In order to study the de-excitation branching in detail, gamma radiation coincident with the appropriate proton groups feeding the states in question was examined with voltage gates set on the proton groups shown in Fig. 5. Figure 11 shows gamma radiation coincident with the groups $p_{1,2}$ and $p_{3,4}$, respectively; these were measured in order to obtain standard spectral shapes to use in analyzing later spectra involving cascade transitions through these states. Figures 12 and 13 show the spectra coincident with p_5 and $p_{9,10}$, respectively. That in coincidence with p_5 clearly shows the direct 8.87-Mev transition, the dominant 2.74–6.13 Mev cascade, and the weaker 1.75–7.12 Mev cascade; the still weaker 1.95–6.92 Mev cascade which appears in the gamma-gamma measurements in II is masked here. The spectrum coincident with $p_{9,10}$ shows the dominant 3.82–7.12 Mev cascade from the 10.94-Mev state as well as the 4.93–6.13 and

[41] A. C. G. Mitchell, in *Beta- and Gamma-Ray spectroscopy*, edited by K. Siegbahn (North-Holland Publishing Company, Amsterdam, 1956).

[42] H. E. Gove and A. E. Litherland (to be published).

[43] Wolicki, Jastrow, and Brooks, Naval Research Laboratory Report NRL-4833, 1956 (unpublished).

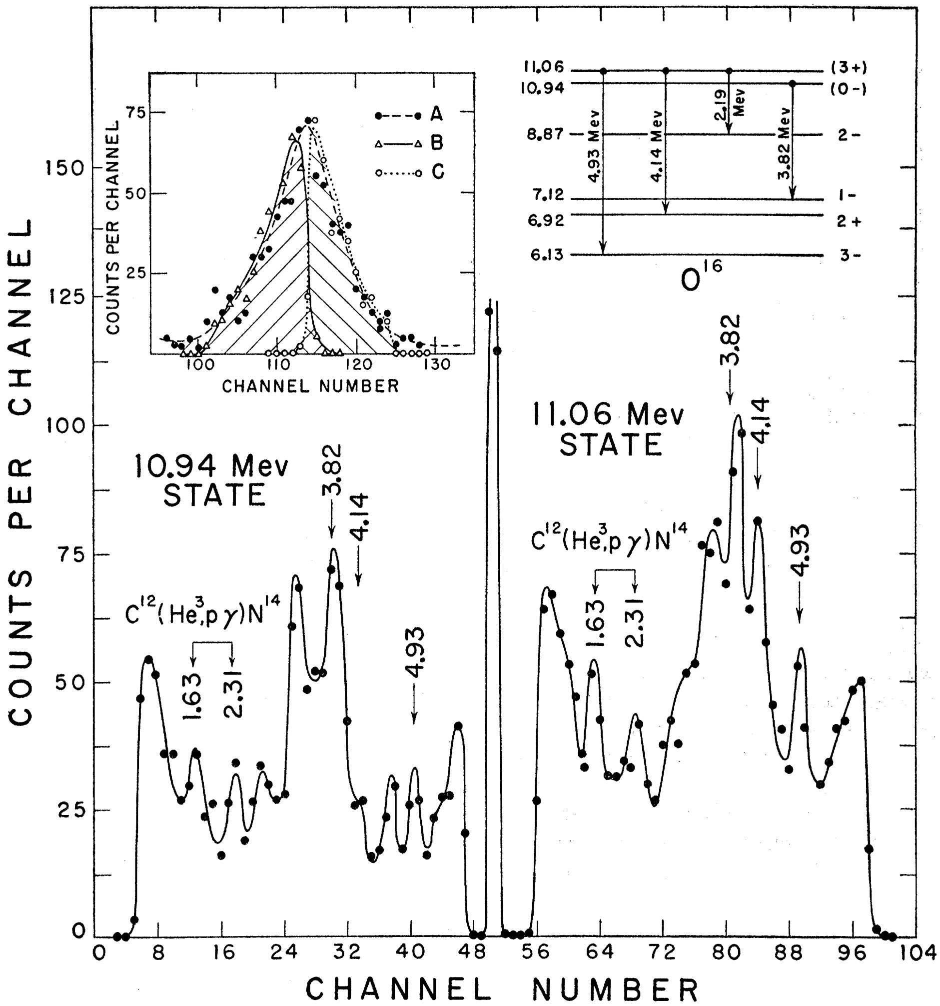

FIG. 14. Use of the PIG circuit in establishing the de-excitation branching from the 10.94- and 11.06-Mev states in O^{16}. Inset is a section of the proton spectrum coincident with gamma radiation (A)—see Fig. 6; showing the two voltage gates B and C set simultaneously on this $p_{9,10}$ peak. Gate C includes predominantly protons to the 10.94-Mev state and B those to the 11.06-Mev state. The gamma transitions involved are shown on the inset level diagrams.

4.14–6.92 Mev cascades from the 11.06-Mev state. The existence of these states corresponding to the unresolved $p_{9,10}$ group is established by the magnet measurements discussed previously. The 2.19-Mev transition from the 11.06- to the 8.87-Mev states is apparent in this figure and does not appear either in the direct spectrum or in the γ-γ coincidence measurements in II because in each case it is masked by a stronger 2.31- or 2.74-Mev transition.

Figure 14, obtained using the PIG circuit previously described,[31] served as a check on the identification of the radiations involved in the de-excitation of the 11-Mev states. As illustrated in the inset figure, voltage gates were set on the upper and lower halves of the unresolved proton group to the 10.94- and 11.06-Mev states measured in coincidence with all gamma radiation with $E_\gamma \gtrsim 700$ kev in a large solid angle CsI detector.[26] The low coincidence efficiency of the Kellogg magnet precluded its use in a coincidence measurement on the resolved groups of Fig. 6, necessitating the use of the CsI detector. The two 50-channel spectra are in coincidence with the voltage gates as shown. The spectrum coincident with the upper energy side of the proton group and consequently predominantly from the lower state at 10.94 Mev shows the 3.82-7.12 Mev cascade strongly, whereas that coincident with the lower energy side and hence from the 11.06-Mev state shows the 4.14–6.92 and 4.93–6.13 Mev cascades.

Figure 15, also obtained with the PIG circuit,[31] shows the simultaneous presentation of the gamma spectra coincident with three different voltage gates set on the output of the proton detector. These proton groups and a typical gate are shown in Fig. 6. The proton detector was set in the plane of the γ counter, i.e., $\theta_p=90°$, $\phi_p=180°$. The separation markers which are the result of the accidental coincidence opening of a gate allowing only the corresponding pedestal to appear on the pulse-height analyzer serve as a check on the resolution spread introduced by the pedestal. The output of a precision mercury relay pulser was used to check the linearity of three pulse channels.[44]

[44] Bromley, Hamann, and Wall, Atomic Energy Commission Report NYO-6543, 1954 (unpublished).

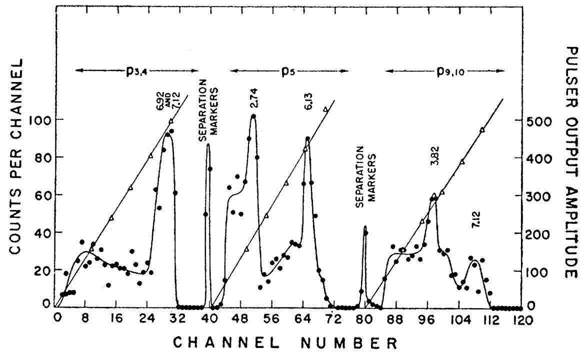

FIG. 15. Use of the PIG circuit in the simultaneous measurement of three ($p\gamma$) coincidence correlations. The voltage gates are set on the proton groups $p_{3,4}$, p_5, and $p_{9,10}$ as in Fig. 6.

Figure 16 shows the angular correlation of the 6.92- and 7.12-Mev complex measured in this way in coincidence with $p_{3,4}$ and that of the 3.82- and 7.12-Mev gamma rays in coincidence with $p_{9,10}$. It should be noted that the 7.12-Mev radiation is observed as the final stage of a (He^3,$p\gamma\gamma$) quadruple correlation with the third radiation unobserved. The intensities involved were not adequate to obtain the correlations for the weaker cascade transitions; however, it was evident from the spectra obtained that none of these had strong correlations. Figure 17 presents the $p\gamma$ correlations for the 1.75-, 2.74-, and 6.13-Mev gamma radiation coincident with p_5; here again the 6.13-Mev radiation is from the quadruple correlation with intermediate radiation unobserved. These data were obtained in a series of measurements using the full 120 channels to display the gamma spectra. The $p\gamma$ correlation measurement measurements have been repeated with the proton detector axis perpendicular to the plane of motion of the gamma detector, i.e., $\theta_p=90°$, $\phi_p=90°$ and isotropic correlations measured in all cases.

The striking feature of all these ($p\gamma$) correlations is their apparent isotropy. The possible consequences of these symmetries will be discussed in detail in II.

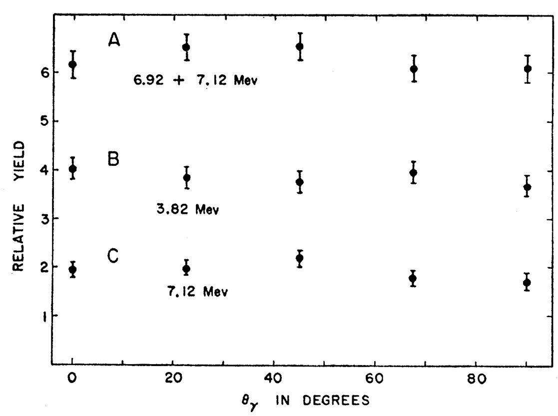

FIG. 16. Proton-gamma angular correlations obtained using the PIG circuit in coincidence with the $p_{3,4}$ group (*A*) and the $p_{9,10}$ group (*B* and *C*).

By fitting standard spectral shapes to the spectra obtained and making use of additional information from the γ-γ measurements of II on the relative intensities of the 1.75–7.12 and 1.95–6.92 Mev cascades from the 8.87-Mev state and of the 4.14–6.92 and 4.93–6.13 cascades from the 11.06 state, the branching ratios shown in Fig. 18 have been obtained. These are also listed in Tables II, III, and IV which will be discussed in the following section.

It has not been possible to carry out measurements on the yield of annihilation radiation, as in the case of He^3 bombardment of C^{12},[26] to obtain values for the cross sections for the $N^{14}(He^3,\alpha)N^{13}$ and $N^{14}(He^3,d)O^{15}$ reactions with significant accuracy, since these activities with half-lives of 10 minutes and 120 seconds, respectively,[5] occur in the presence of the C^{11} and O^{14} activities

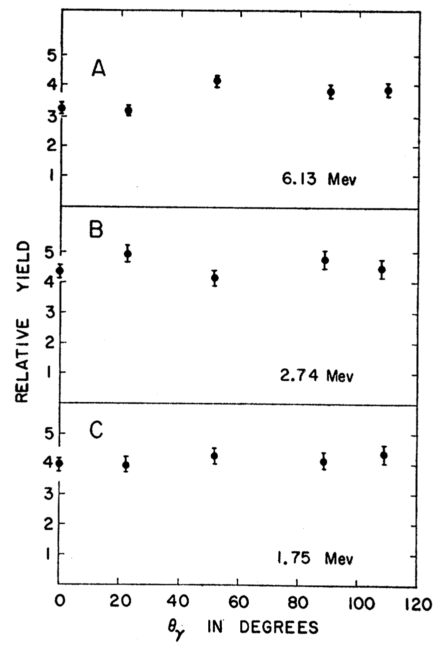

FIG. 17. Proton-gamma angular correlations in the de-excitation of the 8.87-Mev state in O^{16}.

from bombardment of the carbon target contaminant with half-lives of 20 minutes and 72 seconds, respectively.[5]

DISCUSSION

Branching Ratios

The results of the branching ratio measurements are collected in Tables II, III, and IV, for the 8.87, 10.94, and 11.06-Mev states in O^{16}, respectively. Since these states are unbound with respect to alpha emission to C^{12}, the fact that they de-excite via gamma radiation strongly suggests that they all have unnatural parity, i.e., 0^-, 1^+, 2^-, 3^+, etc. To the extent that parity is conserved in strong interactions, these states have vanishing widths for alpha-particle emission to the

TABLE II. De-excitation branching ratios for the 8.87-Mev state in O^{16}. BR$_1$ represents the adjusted and normalized single-particle predictions, BR$_2$ the predictions of the intermediate-coupling calculations,[a] BR$_3$ the experimental results presented herein [N^{14}(He^3,$p\gamma$)O^{16}], BR$_4$ those of Bent and Kruse[b] [F^{19}(p,$\alpha\gamma$)O^{16}], BR$_5$ those of Wilkinson *et al.*[c] [F^{19}(p,$\alpha\gamma$)O^{16} and N^{16}(β^-)O^{16}], and BR$_6$ those of Wakatsuki *et al.*[d] [F^{19}(p,$\alpha\gamma$)O^{16}].

E_γ (Mev)	$(J\pi)_i$	$(J\pi)_f$	Multi-polarity	Γ_w (ev)	BR$_1$	BR$_2$	BR$_3$	BR$_4$	BR$_5$	BR$_6$
8.87	2^-	0^+	$M2$	5.23×10^{-3}	1.70×10^{-2}	5×10^{-2} ($V_c=40$) 17×10^{-2} ($V_c=50$)	9.45×10^{-2}	7.0×10^{-2}	<0.15	9.75×10^{-3}
2.81	2^-	0^+	$M2$	2.67×10^{-7}	5.42×10^{-5}		<0.05			
2.74	2^-	3^-	$M1$ $E2$	0.432 3.04×10^{-4}	1.00	1.00 ($V_c=40$)	1.00	1.00	1.00	1.00
1.95	2^-	2^+	$E1$ $M2$	3.19 2.68×10^{-6}	0.65		6.76×10^{-2}		3.7×10^{-2}	
1.75	2^-	1^-	$M1$ $E2$	0.113 3.23×10^{-5}	0.22	6×10^{-2} ($V_c=40$)	0.189		0.11	

[a] See reference 16. [b] See reference 7. [c] See reference 6. [d] See reference 8.

TABLE III. De-excitation branching ratios for the 10.94-Mev state in O^{16}. See caption to Table II for legend.

E_γ (Mev)	$(J\pi)_i$	$(J\pi)_f$	Multi-polarity	Γ_w (ev)	BR$_1$	BR$_2$	BR$_3$	BR$_4$	BR$_6$
4.02	0^-	2^+	$M2$	1.00×10^{-4}	1.65×10^{-4}		<0.02	<0.2	<0.10
3.82	0^-	1^-	$M1$	1.17	1.00	1.00 ($V_c=40$)	1.00	1.00	1.00
2.07	0^-	2^-	$E2$	7.49×10^{-5}	3.84×10^{-2}	0.03 ($V_c=40$)	<0.05	<0.4	

natural parity states of C^{12}. A survey of the experimental evidence[45] indicates upper limits on the intensity of parity-nonconserving components in these interactions ranging from 1×10^{-4} to 3×10^{-8}. The data presented herein will be examined in this respect later in this section.

Detailed discussion of the 2^- assignment to the 8.87-Mev state has been given by Wilkinson *et al.*[6]; it will be demonstrated in II that the γ-γ angular correlations establish this assignment uniquely.

Since the 10.94-Mev state de-excites almost entirely via a cascade through the 1^-, 7.12-Mev state, an assignment of 0^- is strongly suggested although a 1^+ assignment is not completely excluded. The absence of a ground-state transition from a presumed 1^+ state *a priori* would appear to constitute good evidence against such an assignment. However, as noted by Elliott and Flowers,[16] an $M1$ ground-state transition from a 1^+ state in the vicinity of 11 Mev would be expected to be inhibited by a factor $\sim10^3$, beyond the normal isotopic spin $M1$ inhibition, as a result of the predominantly different wave functions involved. The γ-γ correlation data of II provides additional strong evidence for the correctness of the 0^- assignment; the isotropic angular distribution of the 3.82-Mev gamma radiation is of course consistent with the 0^- assignment but cannot be construed as evidence for this assignment since, as noted previously, all the proton and gamma radiation angular distributions and ($p\gamma$) correlations observed are roughly isotropic. As will be discussed in detail in II, this behavior may well reflect the fact that owing to the high compound-system excitations, sufficient mixing exists to populate equally the magnetic substates of the O^{16} levels involved.

The strong transition from the 11.06-Mev state to the 3^- state at 6.13 Mev and the absence of the ground-state transition constitute evidence against assignments of 0^- or 1^+, respectively; that to the 2^+ state at 6.92 Mev makes a 4^+ or higher spin assignment highly improbable, leaving 2^- and 3^+ as reasonable possibilities. The γ-γ angular correlations, while suggesting 3^+, do not completely preclude the possibility of 2^-. Table IV therefore includes both possibilities.

The tabulated transition widths Γ_w are the usual Weisskopf extreme-single-particle values[46] calculated for the indicated transitions. In the case of O^{16}, these

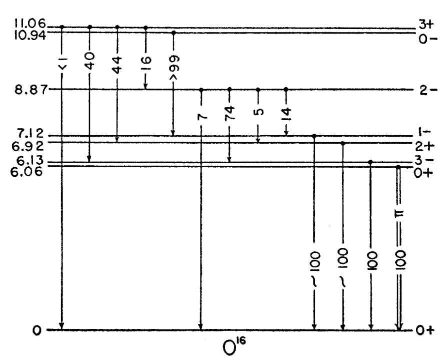

FIG. 18. Relative de-excitation widths for the 8.87-, 10.94-, and 11.06-Mev states in O^{16}.

[45] D. H. Wilkinson, in *Proceedings of the Rehovoth Conference on Nuclear Structure*, edited H. J. Lipkin (North-Holland Publishing Company, Amsterdam, 1958); Phys. Rev. **109**, 1603, 1610 and 1614 (1958).

[46] D. H. Wilkinson, Atomic Energy Research Establishment Report T/R 2492, 1958 (unpublished).

TABLE IV. De-excitation branching ratios for the 11.06-Mev state in O^{16} assuming both 3^+ and 2^- assignments for comparison. See caption to Table II for legend.

E_γ (Mev)	$(J\pi)_i$	$(J\pi)_f$	Multi-polarity	Γ_w	BR_1	BR_3	BR_6
11.06	3^+	0^+	$M3$	5.53×10^{-6}	5.71×10^{-6}	<0.02	$\sim4\times10^{-3}$
4.93	3^+	3^-	$E1$	51.52	2.66	0.91	1.00
			$M2$	2.77×10^{-4}			
4.14	3^+	2^+	$M1$	1.49	1.00	1.00	
			$E2$	2.40×10^{-3}			
3.94	3^+	1^-	$M2$	9.04×10^{-5}	7.43×10^{-5}	<0.05	
2.19	3^+	2^-	$E1$	4.52	0.232	0.36	
			$M2$	4.80×10^{-6}			
11.06	2^-	0^+	$M2$	1.57×10^{-3}	8.69×10^{-4}	<0.02	$\sim4\times10^{-3}$
4.93	2^-	3^-	$M1$	2.52	0.698	0.91	1.00
			$E2$	5.74×10^{-5}			
4.14	2^-	2^+	$E1$	30.5	1.00	1.00	
			$M2$	1.16×10^{-4}			
3.94	2^-	1^-	$M1$	1.28	0.646	<0.05	
			$E2$	1.87×10^{-3}			
2.19	2^-	2^-	$M1$	0.220	7.64×10^{-2}	0.36	
			$E2$	1.00×10^{-4}			

have the numerical values, for $r=(1.5 \text{ fermis})A^{\frac{1}{3}}$,

$$\Gamma_{E1}=0.43E_\gamma^3, \qquad \Gamma_{M1}=0.021E_\gamma^3,$$
$$\Gamma_{E2}=1.97\times10^{-6}E_\gamma^5, \qquad \Gamma_{M2}=9.52\times10^{-8}E_\gamma^5,$$
$$\Gamma_{E3}=5.89\times10^{-12}E_\gamma^7, \qquad \Gamma_{M3}=2.74\times10^{-13}E_\gamma^7,$$

where $\Gamma_{E\lambda}$ is expressed in ev and E_γ in Mev.

Since the lowest $T=1$ level in O^{16} corresponding to the ground state of N^{16} is at 13 Mev,[5] all the states considered in this study have predominantly $T=0$. Consequently, because of the self-conjugate nature of this nucleus it would be expected that the usual isobaric spin inhibition factors would apply to $E1$ transitions[47]; similarly the magnetic transitions are inhibited as discussed recently by Morpurgo[48] and Warburton.[49] $E2$ transitions, on the other hand, would be expected to be enhanced by collective effects represented by effective neutron charge. In the discussion to follow, the possibility of appreciable isobaric impurities in the states involved has been ignored; the presence of the 2^- and 0^-, $T=1$ analogs of the N^{16} ground state and first excited state[50] at $\sim$13 Mev in O^{16} will of course result in finite, albeit small, $T=1$ mixing into the 8.87- and 10.94-Mev states. Wilkinson[50] has estimated that in the case of the 8.87-Mev state $10^{-3}<\alpha^2(1)<0.03$, with the lower limit favored, where $\alpha^2(1)$ is the relative intensity of the $T=1$ admixture in this state. The location of the first 3^+ $T=1$ state in O^{16} has not been established.

The geometric mean of the inhibition factors, as compared to the Weisskopf widths, tabulated by Wilkinson[45] for isotopic spin forbidden $E1$ transitions, is $\sim0.75\times10^{-3}$; and for purposes of comparison in this paper a value of 10^{-3} has been chosen. The inhibition factor for magnetic transitions ($M\lambda$) is given by[48,49]

$$\left\{\frac{\mu_p+\mu_n+G/(\lambda+1)}{\mu_p-\mu_n-G/(\lambda+1)}\right\}^2 =8.3\times10^{-3} \text{ for } M1 \text{ transitions}$$
$$=1.6\times10^{-2} \text{ for } M2 \text{ transitions}$$
$$=2.0\times10^{-2} \text{ for } M3 \text{ transitions,}$$

on the assumption that $G=-1$, the statistical mean value.

If an effective charge αe is assumed for the neutron and $(1+\alpha)e$ for the protons, to take into account the core recoil, then the quadrupole moment $Q\sim(1+2\alpha)e$ for $T=0$ transitions and the enhancement factor for $E2$ transitions is then $(1+2\alpha)^2$. From the mean life of the $E2$ de-excitation of the 872-kev state of O^{17} of $(2.5\pm1)\times10^{-10}$ second[51] and the rms nuclear radii as measured by high-energy electron scattering,[52] a value of $\alpha=0.64\pm0.16$ is obtained, giving an enhancement factor equal to 5.2 ± 1.5. This is in good accord with calculations of Barker[53] for the $E2$ enhancements to be expected for $A=18$ and $A=19$. A factor of 5.0 has been assumed for convenience.

Applying these correction factors to the Weisskopf widths listed in the tables and expressing the total width for each component relative to that of the most intense in the observed spectra, the branching ratios BR_1 are obtained as the corrected single-particle predictions. BR_2 lists the available branching-ratio predictions from the intermediate-coupling shell-model calculations of Elliott and Flowers.[16] BR_3 lists the experimental branching ratios obtained here in the $N^{14}(He^3,p\gamma)O^{16}$ measurements; BR_4 lists those of Bent and Kruse[7]; BR_5, those of Wilkinson, Toppel, and Alburger[6]; and BR_6 those of Wakatsuki *et al.*[8]

[47] M. Gell-Mann and V. L. Telegdi, Phys. Rev. **91**, 169 (1953).
[48] G. Morpurgo, Phys. Rev. **110**, 721 (1958).
[49] G. K. Warburton, Phys. Rev. Letters **1**, 68 (1958).
[50] W. Zimmerman, Phys. Rev. **104**, 387 (1956). See also D. H. Wilkinson, Phil. Mag. **1**, 379 (1956).
[51] J. Thirion and V. L. Telegdi, Phys. Rev. **92**, 1253 (1953).
[52] R. Hofstadter, Revs. Modern Phys. **28**, 214 (1956).
[53] F. C. Barker, Phil. Mag. **1**, 329 (1956).

The data in Table II are in accord with the 2^- assignment to the 8.87-Mev state. Those in Table III strongly suggest a 0^- assignment but cannot exclude 1^+ completely. Assignments of 2^-, 3^+ or higher are excluded, however.

It is of interest to note that the 11.06-Mev state appears to be fed very weakly, if at all, by the $N^{15}(d,n\gamma)O^{16}$ and $F^{19}(p,\alpha\gamma)O^{16}$ reactions. The numbers quoted for BR_6 for the 11.06 state are very approximate and were obtained from relative intensity estimates given by Wakatsuki *et al.*[8] As shown in Table IV, the branching ratios reported in this paper for the 11.06-, 4.93-, and 4.14-Mev transitions are in roughly equally good accord with either a 2^- or 3^+ assignment for the 11.06-Mev state. On the other hand, those for the 3.94- and 2.19-Mev transitions favor the assignment 3^+ by at least an order of magnitude in both cases. Spin and parity assignments based on branching ratios alone are highly suspect, however; additional evidence suggesting the correctness of the 3^+ assignment will be adduced in II.

In these tables the branching ratio data from different sources show quite satisfactory internal consistency, the largest discrepancy being a factor ~ 2 in Table II. Again with the exception of this transition, the measured branching ratios accord remarkably well with the adjusted single-particle values for the assignments quoted.

Parity Impurities

From the observation of gamma radiation from the unnatural parity states in O^{16}, it is possible to arrive at an estimate of the $\Gamma_\alpha/\Gamma_\gamma$ branching from the 10.94-Mev state and thus of an upper limit on the intensity of the opposite-parity components in the wave function for this state. Because the proton group feeding the state is not clearly resolved in the direct spectrum, an indirect measurement of $\Gamma_\alpha/\Gamma_\gamma$ has been necessary. From magnetic spectrometer measurements such as those shown in Fig. 7, it has been possible to determine the relative cross sections for formation of the states in the region of 11-Mev excitation and thus the fraction of the total counts in the voltage gate set on this section of the direct spectrum which are attributable to the formation of the 10.94-Mev state. From $(p\gamma)$ coincidence spectra such as that shown in Fig. 13, measured in coincidence with this voltage gate, the corresponding yield of 3.82-Mev de-excitation radiation from the 10.94-Mev state was obtained. The predicted yield of this radiation is given in terms of the number of coincident proton counts, the measured efficiency of the gamma spectrometer at this energy, and the de-excitation branching ratio as

$$N_\gamma = N_p \epsilon_\gamma [\Gamma_\gamma/(\Gamma_\alpha+\Gamma_\gamma)],$$

and the experimental value for the branching ratio is given by

$$\frac{\Gamma_\gamma}{\Gamma_\alpha+\Gamma_\gamma} = \frac{N_\gamma(\text{experimental})}{N_p(\text{experimental})\epsilon_\gamma}.$$

From the experimental data $\Gamma_\gamma/(\Gamma_\alpha+\Gamma_\gamma)$ was obtained as 1.1 ± 0.3, which would be consistent with $\Gamma_\alpha/\Gamma_\gamma \sim 0$. For purposes of discussion, a value of $\Gamma_\alpha/\Gamma_\gamma \leq 0.20$ has been used.

If the wave function for the 10.94-Mev state is written as

$$\psi_0 = \alpha\psi_{0-} + \beta\psi_{0+},$$

then an estimate of the upper limit on the intensity of the opposite parity component, $(\beta/\alpha)^2$, follows from

$$(\beta/\alpha)^2 = (\Gamma_\gamma/\Gamma_\alpha')(\Gamma_\alpha/\Gamma_\gamma),$$

where parity impurities in the 7.12-Mev state of O^{16} and the ground state of C^{12} are considered negligible and where Γ_γ is the width for $M1$ de-excitation of the state via a cascade transition to the 7.12-Mev state, Γ_α' is the width which would be appropriate to the s-wave alpha de-excitation of a natural parity state at 10.94 Mev in O^{16}, and Γ_α the actual width for alpha decay of the state.

From Wilkinson's compilation,[45] normal alpha-particle reduced widths center on a value of 0.05 single-particle unit. As noted previously, an isobaric spin inhibition factor $\sim 8\times10^{-3}$ applies to $M1$ gamma radiation widths in O^{16} [48,49]; Wilkinson[45] suggests that the most probable value for $M1$ widths is ~ 0.15 Weisskopf unit. From Table III, Γ_w for the 3.82-Mev $M1$ transition is 1.17 ev; assuming $r_0 = 1.45(A_1^{\frac{1}{3}}+A_2^{\frac{1}{3}})$ fermis in accord with available scattering data,[54] the single-particle alpha reduced width is $\gamma_{sp}^2 = \hbar^2/MR^2 \approx 500$ kev and, for assumed S wave α de-excitation to the C^{12} ground state,

$$\Gamma_\alpha' = \frac{2\rho}{F_0^2+G_0^0}(0.05\gamma_{sp}^2) \approx 200 \text{ kev.}^{55}$$

Inserting the values in the expression given above for $(\beta/\alpha)^2$ results in an upper limit estimate of

$$(\beta/\alpha)^2 \leq 2\times10^{-9}.$$

It should be emphasized that, in view of the assumptions made in arriving at this limit, it should not be considered as established to better than an order of magnitude at most. This estimate is obtained for the 10.94-Mev state; less stringent limits follow for the 8.87- and 11.06-Mev states, since in these cases the more complex gamma de-excitation results in a less direct extraction of a limit. It is interesting to note that this estimate is quite consistent with the limit of 4×10^{-8} previously

[54] Kerlee, Blair, and Farwell, Phys. Rev. **107**, 1343 (1957). J. S. Blair, Phys. Rev. **108**, 827 (1957).

[55] I. Bloch *et al.*, Revs. Modern Phys. **23**, 147 (1951); Sharp, Gove, and Paul, Chalk River Report TPI-70, 1953 (unpublished).

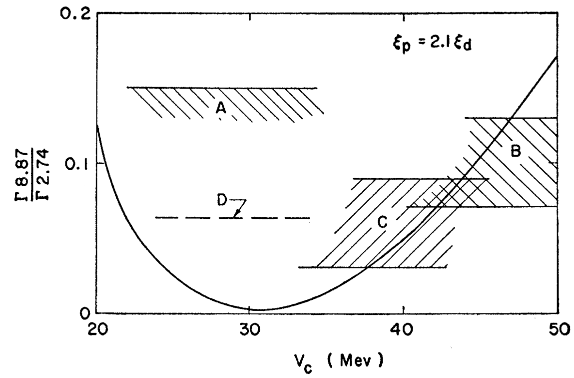

FIG. 19. Comparison of the relative widths for 8.87- and 2.74-Mev transitions from the 8.87-Mev state in O^{16} with the intermediate-coupling shell-model calculations. A represents the upper limit established in reference 6, B is the result reported in this paper, C is that of reference 7, and D that of reference 8. V_c is the depth of the central potential assumed in the calculations.

obtained.[45] The estimate of 3×10^{-8} obtained by Wilkinson[56] for this limit, using the $F^{19}(p,\gamma\gamma)O^{16}$ (7.12 Mev) reaction, does not include an estimate of the $M1$ inhibition factor to be expected for $\Delta T=0$ transitions in O^{16}.[48] Assuming a value of 100 for this inhibition, the quoted limit is increased to $\sim3\times10^{-6}$. A much less stringent limit is established by the previously noted nonobservation of de-excitation gamma radiaton from the 4^+, 10.36-Mev state in O^{16} populated in the $N^{14}(He^3,p)O^{16}$ reaction.

Intermediate-Coupling Shell Model

Figure 19 shows in more detail the comparison of the 8.87/2.74 branching ratio with the predictions of Elliott and Flowers.[6] In this plot, V_c is the depth of the central potential assumed in the calculations; the ratio of p to d shell spin-orbit-energy splitting has been fixed at 2.1 as determined from the O^{15}, N^{15}, and O^{17} level spectra. The branching ratio reported here corresponds to $43\leq V_c\leq47$ whereas that of Bent and Kruse[7] corresponds to $38\leq V_c\leq44$, suggesting a value $V_c=43$–44 Mev. This is in excellent agreement with $V_c=43$ Mev which is required to give the correct separation between the ground and 3^-, 6.13-Mev level in O^{16},[16] the binding energy of the deuteron, and the level spectra in the mass 18[38,57,58] and 19[59] systems as calculated using a similar model by Elliott and Flowers.[60] It should be noted, however, that a value $V_c\sim20$ Mev is not excluded by this figure.

Elliott and Flowers state that the predicted 1.75/2.74 branching ratio of 6×10^{-2} is remarkably independent of both V_c and the ratio of the spin-orbit splittings assumed; it is in disagreement with the experimental values by a factor ~3. These authors note, moreover, that the 1^-, 7.12-Mev state involved here has large admixtures of higher configurations which would reduce the predicted branching ratio even further. On the other hand, it should be emphasized that in the calculations an almost pure E2 transition is indicated for the 1.75-Mev radiaton and a mixed $M1$-$E2$ transition for the 2.74-Mev radiation. Elliott[61] notes that since the same effective charge was assumed for both p and ds particles, $E2$ widths of transition involving the p particles may well have been overestimated in the original calculations by factors perhaps up to 4 and that this effect would reduce the predicted branching ratio in the direction to bring it into accord with experiment.

The branching ratios predicted by the intermediate-coupling model for the de-excitation of the 10.94-Mev state, with a 0^- assignment, are shown in Table III (BR_2)[61] and are in accord with the observations. With a 0^- assignment to this state, it is possible to fix the exchange mixture in the potential appropriate to the O^{16} calculation with considerable accuracy. Elliott and Flowers[16] have used the Rosenfeld l mixture with Wigner, Majorana, Heisenberg, and Bartlett force amplitudes $W=0.13$, $M=-0.93$, $H=0.26$ and $B=-0.46$ in all the (sd) shell calculations.[16,53] In addition to the usual convention $W+M+H+B=-1$, comparison of the $A=18$ and 19 calculations with the experimental data fixed $W+M-H-B=-0.7$ and $W-M-H+B=0.26$ with $V_c=43$ Mev as selected earlier. Using these restrictions, the exchange mixture may be expressed in terms of the singlet-singlet interaction, $x=W-M+H-B$. When the negative-parity level spectrum for O^{16} is calculated as a function of x, Elliott and Flowers[16] find that only the 0^- states have strong dependence on the value of x; the lowest 0^- predicted excitation ranges from ~10.3 to 15 Mev for $-3\leq x\leq+3$. From the location of the 0^- level at 10.94 Mev, it follows that $W\approx M\approx0.4$, $B\approx-0.1$ and $H\approx0.2$. This result is very similar to that found by Soper[62] in fitting the first six levels of Li^6, namely $W\approx0.4$, $M\approx0.3$, $B\approx0.2$, and $H\approx0.1$; both are much closer to the Serber mixture, $W=M=0.5$, than to the Rosenfeld mixture normally assumed. Use of the "O^{16} mixture" may have interesting consequences in further detailed shell model calculations; specifically it is known that an exchange mixture close to a Serber one appears to be required to give the proper relative $T=1$ and $T=0$ level spacings in F^{18}.[58]

It may be concluded from the results presented here and others to be presented in II that the intermediate-coupling shell model calculations, where applicable, give a satisfactory representation of the experimental data. It should be noted, however, that the 1^- state at

[56] N. Tanner, Phys. Rev. **107**, 1203 (1958).
[57] Kuehner, Almqvist, and Bromley, Bull. Am. Phys. Soc. Ser. II, **3**, 27 (1958), and to be published.
[58] Bromley, Kuehner, and Almqvist, Bull. Am. Phys. Soc. Ser. II, **3**, 27 (1958), and to be published.
[59] E. B. Paul, Phil. Mag. **2**, 311 (1957).
[60] J. P. Elliott and B. H. Flowers, Proc. Roy. Soc. London **A229**, 536 (1955).
[61] J. P. Elliott (private communication, 1958).
[62] J. M. Soper, Phil. Mag. **2**, 1219 (1957).

9.58 Mev identified in the $C^{12}(\alpha,\alpha)C^{12}$ measurements of Hill[63] has no counterpart in the predicted level spectrum, the second 1^- being predicted at 16.5 Mev.

It may perhaps be significant, however, that the intermediate-coupling calculations both for[16] O^{16} and for[60,64] F^{18} predict, in general, the correct ordering for the levels in these nuclei although the excitation energies predicted are not in accord with the experimentally observed spectra at values of the intermediate-coupling parameters consistent with other data, i.e., $V_c \approx 40$ Mev in Elliott and Flowers calculations. In the O^{16} case a multiplicative factor of 0.85 applied to the predicted excitations achieves quite good agreement for the 3^-, 1^-, 2^-, and 0^- states at 6.13, 7.12, 8.87, and 10.94 Mev, respectively. The additional 1^- state at 9.58 Mev as noted is not predicted by the calculations.

In the F^{18} calculations of Redlich[64] a similar multiplicative factor of 0.58 is required to obtain agreement with the observed spectrum.[58] In those of Elliott and Flowers,[60] no such simple factor suffices; however, it has been noted by Elliott[65] that inclusion of the previously neglected surface-particle coupling terms appropriate to the quadrupole moment of O^{17} brings the predicted spectrum into reasonable agreement with that observed without destroying the previously obtained agreement in the case of F^{19}.[59]

Alpha-Particle Model

No detailed calculations of transition widths have been carried out within the framework of the O^{16} alpha-particle model. The integrals involved in these calculations are in many instances intractable[66]; because of other more obvious discrepancies it has not been considered worthwhile to investigate this problem in detail. The most recent study of this model is that of Kameny,[15] based on the original Dennison[13] model and identifications.[14] On identification (a) (based on the O^{16} states at 0, 6.06, 6.13, 7.12, and 9.84 Mev) the lowest predicted 0^- state is at 20.31 Mev. The identification of the 10.94-Mev state makes this assignment untenable, contrary to the original indications favoring (a) over (b). On identification (b) (based on the O^{16} states at 0, 6.06, 6.13, 6.92, and 7.12 Mev) the lowest 0^- state is predicted at 11.52 Mev. Since, in 0^{16}, the Coulomb forces would be expected to depress 0^- and 1^- states relative to 2^- and 3^+,[65] this prediction accords well with experiment. This model, predicts a $2^{\mp}$ doublet in the vicinity of 12.97 Mev and the lowest 3^+ level at 11.72 Mev. Both a "tunneling" correction[14] corresponding to the interchange of 2 of the 4 alpha particles and the Coulomb corrections would be expected to increase the 2^- excitation relative to the 2^+, suggesting that the 2^+ and 2^- states at 11.51 and 12.51 or 12.95, respectively, may represent this doublet. Consequently an assignment of 3^+ rather than 2^- to the level at 11.06 Mev would be in considerably better agreement with the alpha model.

On identification (b), a $2^{\mp}$ parity doublet is fixed by the base 2^+ level at 6.92 Mev. Although in this case also the "tunneling" energy would be expected to split the doublet with the 2^- state at the higher excitation, Dennison[14] has estimated that the splitting should be in the kev region and thus inadequate to account for the presence of the 2^-, 8.87-Mev level. This discrepancy is a serious one and despite the rather remarkable agreement obtained with the model in fitting other levels in the spectrum, suggests that it should be applied with considerable caution. Further work such as that of Perring and Skyrme[17] on the fundamental connections between the alpha-particle and shell models will be of great interest.

Collective Model

The calculations to date on the collective models for the positive-parity states in O^{16} have been carried out on a restricted basis with major emphasis on the properties of the 0^+ state at 6.06 Mev. All models which have been suggested to date[18–21] appear to be unable to predict a lifetime for this state in agreement with the experimental data. Nor does it appear possible to accommodate the higher level spectrum within the framework of any of the existing models, all of which predict much higher excitations for the 2^+ and 4^+ levels than would be consistent with experiment. The possibility that the predicted levels are indeed present at higher excitations and that the lower levels represent more complex configurations cannot be excluded.

CONCLUSION

To conclude therefore, the observed unnatural parity levels and their de-excitation in O^{16} eliminate the alpha-particle model identification (a) previously favored,[14] leaving identification (b); while accounting for the 10.94- and 11.06-Mev levels in satisfactory fashion, this model has the serious discrepancy of omitting the level at 8.87 Mev. The O^{16} exchange mixture is determined as much more similar to the Serber than to the Rosenfeld mixture normally used; the intermediate- coupling shell-model calculations give an adequate representation of the present data although there are remaining discrepancies in the level spectrum involving the location of the anomalous 1^- levels.[63,5] The experimental results reported here do not bear directly on the validity of the collective model for O^{16}. In all three models there are areas of agreement and in the case of the alpha-particle and intermediate-coupling shell models, isolated, but perhaps serious discrepancies. The most reasonable conclusion would appear to be that a complete description of the O^{16} leve

[63] R. W. Hill, Phys. Rev. **90**, 845 (1953).
[64] M. G. Redlich, Phys. Rev. **95**, 448 (1954); **110**, 468 (1958); and private communication, 1958.
[65] J. P. Elliott (private communication, 1957).
[66] J. Scott-Thomas (private communication, 1958).

spectrum is not yet available; aspects of all three models may be required in the more complete treatment and theoretical treatment of the connections between the models[17,67,68] may well suggest the required modifications. In the case of the 10.94-Mev level, the observation of gamma de-excitation in competition with the energetically possible alpha emission to C^{12} permits an estimate of an upper limit on the relative intensity of the opposite-parity component in the state wave function $\sim 2\times 10^{-9}$.

ACKNOWLEDGMENTS

We are indebted to Dr. G. A. Bartholomew, Dr. J. P. Elliott, and Dr. R. A. Ferrell, for interesting discussions regarding this work, to Mr. W. Woytowich for his assistance in developing the target production techniques, and to Mr. P. G. Ashbaugh and his group for operation of the accelerator.

APPENDIX I. SUMMATION CORRECTIONS

In obtaining relative intensities of weak gamma radiations in direct spectra, it is essential that corrections be applied for summation contributions to the full-energy pulse-height region resulting from simultaneous detection of two cascade gamma radiations from the level in question in a single crystal with a resultant full-energy pulse. In the direct spectra such pulses are indistinguishable from those corresponding to a ground-state de-excitation transition from this level.

As noted in the text, these contributions are clearly functions both of the effective solid angle of the detectors and of the γ-γ angular correlations for the cascade radiations; thus the summation contributions vanish if the radiations are uniquely correlated at 180° and are maximum for a 0° correlation.

If an isotropic γ-γ correlation is assumed, the summation contribution is given simply by

$$S_0 = N\epsilon_{\gamma 1}\epsilon_{\gamma 2},$$

where N is the number of times the level in question is formed and ϵ_γ is the detector efficiency for the radiation energies involved. For a nonisotropic γ-γ correlation this becomes

$$S = N\epsilon_{\gamma 1}\epsilon_{\gamma 2}R,$$

where the correction factor R is a function of the coefficients in the γ-γ correlation. The functional form of R is obtained as the ratio of the γ-γ correlation averaged over the effective detector aperture to its average over the sphere.

In general, however, the γ-γ correlations (as in II for example) are measured with one gamma detector fixed at 90° to the incident beam and the other variable in angle; the correlations as quoted are expressed in terms of Legendre polynomials of the angle θ between the moving counter and the beam direction:

$$W_{\gamma,\gamma}(\theta) = \sum_n a_{2n}P_{2n}(\cos\theta).$$

In obtaining R, however, the correlation is required as a function of the angle $\phi = \theta + 90°$ between the gamma detectors and a simple substitution gives

$$W_{\gamma,\gamma}'(\phi) = \sum_n b_{2n}P_{2n}(\cos\phi),$$

whence

$$R = \left(\int_1^{\cos\theta_0} W_{\gamma,\gamma}'(\phi)d(\cos\phi) \Big/ \int_1^0 W_{\gamma,\gamma}'(\phi)d(\cos\phi) \right) \times (1-\cos\theta_0)^{-1},$$

where θ_0 is the half-angle of the effective angular acceptance of the gamma detector.

Carrying out these integrations on the assumption that $n \leq 2$ and substituting in terms of the original γ-γ correlation expansion coefficients a_0, a_2, and a_4 results in

$$R = \frac{8+8x+23y-(12x+40y)f(\theta_0)-35y\times g(\theta_0)}{(8+4x+16.67y)},$$

where

$$f(\theta) = \tfrac{1}{3}(1-\cos^3\theta)/(1-\cos\theta),$$
$$g(\theta) = \tfrac{1}{5}(1-\cos^5\theta)/(1-\cos\theta),$$
$$x = a_2/a_0, \quad y = a_4/a_0.$$

In this expression it has been assumed that the circular cross section of the crystal spectrometer could be adequately approximated by an equivalent rectangular aperture; the integrations over solid angles are, of course, much more complex without this approximation and the error introduced by it is much smaller than the statistical errors involved. The effective aperture is clearly a function of the gamma radiation energy. As a working rule, it has been found convenient to use an aperture of lateral dimensions equal to the crystal diameter less twice the radiation length corresponding to the radiation in question.

---

[67] J. P. Elliott, Proc. Roy. Soc. London **A245**, 128 (1958), Part I.

[68] J. P. Elliott, Proc. Roy. Soc. London **A245**, 562 (1958), Part II.